



ELSEVIER

Contents lists available at ScienceDirect

Journal of Magnetic Resonance

journal homepage: www.elsevier.com/locate/jmr

Communication

Quick, sensitive serial NMR experiments with Radon transform

Rupashree Dass ^b, Paweł Kasprzak ^a, Krzysztof Kazimierczuk ^{b,*}^aDepartment of Mathematical Methods in Physics, Faculty of Physics, University of Warsaw, Pasteura 5, Warsaw, Poland^bCentre of New Technologies, University of Warsaw, Banacha 2C, 02-097 Warsaw, Poland

ARTICLE INFO

Article history:

Received 15 June 2017

Revised 17 July 2017

Accepted 29 July 2017

Available online 31 July 2017

Keywords:

Radon transform

Multidimensional spectroscopy

HSQC

Variable temperature

ABSTRACT

The Radon transform is a potentially powerful tool for processing the data from serial spectroscopic experiments. It makes it possible to decode the rate at which frequencies of spectral peaks shift under the effect of changing conditions, such as temperature, pH, or solvent. In this paper we show how it also improves speed and sensitivity, especially in multidimensional experiments. This is particularly important in the case of low-sensitivity techniques, such as NMR spectroscopy. As an example, we demonstrate how Radon transform processing allows serial measurements of ¹⁵N-HSQC spectra of unlabelled peptides that would otherwise be infeasible.

© 2017 Elsevier Inc. All rights reserved.

1. Introduction

NMR spectroscopy is one of the most powerful tools that exists in analytical chemistry. Several improvements over the decades have contributed to its efficiency. In the 1960s Ernst showed how it was possible to increase speed and sensitivity by performing the acquisition of a free induction decay signal (FID) in time domain, and processing it by Fourier transform (FT) to get the spectrum [1]. This discovery opened the way to multidimensional (ND) spectroscopy, first proposed by Jeener [2] and Ernst [3]. In ND NMR one acquires a signal that is a function of multiple time variables, and which contains information on interactions between nuclei or events that occur during the “additional” (or “indirect”) times that correspond to delays in a sequence of magnetic pulses exciting a sample. Although the indirect dimensions are usually processed with FT, numerous techniques exist where other transforms can be used. The most common of these alternative techniques uses inverse Laplace transform to decode exponential decay coefficients that correspond to diffusion [4] or relaxation [5] rates. Recently, Kupče and Freeman have proposed the use of Radon transform (RT) (in the experimental technique referred to as PROSPECT) to decode the rate of linear change of peak positions caused by variations in temperature, pH, solvent, molecular binding, and other factors [6]. The same authors introduced RT into ND NMR [7] and it was also used in many other applications [8]. However, despite its potential to improve the speed and sensitivity of serial NMR measurements, the work of these authors seems to have attracted

little attention – perhaps because the authors only very briefly mention speed and sensitivity. In this paper we try to show how the use of RT enables quick, sensitive experiments, and how it can be extended into higher dimensions where the benefits are even more pronounced.

2. The Radon transform

The principle of RT processing of series of FID signals $f(s, t)$ (s enumerates the experiments, t is time) is explained in detail by Kupče and Freeman [6]. Their implementation of RT is given by the formula:

$$R(\omega, \varpi) = \int \hat{f}(s, \omega + \varpi \cdot s) ds \quad (1)$$

(here \hat{f} stands for FT over t , ω stands for the frequency and ϖ for its rate of change). Replacing \hat{f} with

$$\hat{f}(s, \omega) = \int f(s, t) \exp(-2\pi i t \omega) dt \quad (2)$$

in (1) we can write $R(\omega, \varpi)$ in the form which resembles FT, with an additional degree of freedom:

$$R(\omega, \varpi) = \iint f(s, t) \exp(-2\pi i t (\omega + \varpi \cdot s)) ds dt. \quad (3)$$

While standard FT attempts to find the frequencies present in a single signal, RT additionally looks for the rate of change of these frequencies from one FID to another in a series. In FT the signal is multiplied by a set of oscillatory functions and the product is

* Corresponding author.

E-mail address: k.kazimierczuk@cent.uw.edu.pl (K. Kazimierczuk).

integrated, providing a non-zero result (“peak”) if a given “test frequency” is present in the signal. In RT various “rates of change” (ϖ) are additionally tested for every frequency ω . The result is a two-dimensional spectrum that contains peaks indicating the frequencies of components, as well as their rates of change. The shape of the peaks in Radon spectra is discussed by Kupče and Freeman [6]. In the SI to the present paper, we derive its exact analytical form and present MATLAB script for simulations. The formula for the real part of the lineshape $R(\omega, \varpi)$ assigned to the series of Lorentzian peaks with the rate of change ϖ_0 , initially centred at zero frequency, each being of width $\Delta\varpi_{1/2}$ with $s \in [0, M]$ is:

$$\begin{cases} \frac{1}{2\pi(\varpi - \varpi_0)} \arg\left(\frac{\omega - i\Delta\varpi_{1/2} + (\varpi - \varpi_0)M}{\omega - i\Delta\varpi_{1/2}}\right) & \text{if } \varpi \neq \varpi_0 \\ \frac{1}{2\pi} \frac{M\Delta\varpi_{1/2}}{\varpi^2 + \Delta\varpi_{1/2}^2} & \text{if } \varpi = \varpi_0 \end{cases} \quad (4)$$

where \arg is the function of complex variable $z = |z|e^{i\varphi}$ $\varphi \in [0, 2\pi]$, which is defined by $\arg(z) = \varphi$.

Formula (3) can be naturally extended to the context of multidimensional NMR. In this case the series of FID signals is represented by a function $f(s, \vec{t})$, where $s \in [0, M]$, $\vec{t} \in \mathbb{R}^n$ and the Radon transform of f is defined by

$$R(\vec{\omega}, \vec{\varpi}) = \int f(s, \vec{t}) \exp(-2\pi i \vec{t} \cdot (\vec{\omega} + s\vec{\varpi})) ds d^n \vec{t}. \quad (5)$$

Lineshapes in RT spectra have several interesting features that are not mentioned in the original paper [6]. First, the number of FIDs in a series determines the resolution (linewidth) in the ϖ dimension (see Fig. 1 panels A,B and C). Secondly, the linewidth in ω dimension influences the linewidth in ϖ dimension (see Fig. 1 panels D,E and F). Both these facts can be understood by considering Formula (3) for a signal in which peak moves from FID to FID at the rate ϖ_0 , with no change of intensity. When ϖ matches the rate of change of a given spectral frequency (ϖ_0), the $R(\omega, \varpi_0)$ cross-section contains a standard NMR peak (usually Lorentzian) centred at ω_0 . The peak is N times higher than it would be in each of the spectra separately. On the other hand, far from the matching condition ($\varpi \ll \varpi_0$ or $\varpi \gg \varpi_0$) the cross-section $R(\omega, \varpi)$ is a series of separated peaks. The narrower the linewidth in ω the sooner peaks separate in ϖ dimension. A third important observation about lineshape is that the shape of the “shoulders” of the peak indicates changes of intensity that occur in parallel to the shift (see Fig. 1 panels G,H and I). SI contains script generating Fig. 1.

For RT it is necessary to define a grid in the ϖ dimension – both the maximum scale and the mesh size. Unlike with FT, these are not defined by sampling: both are post-acquisition parameters

and thus the experiment is not prone to mis-setting. Given the above considerations about lineshape, the only recommendation is to acquire as many spectra as possible, with lowest possible number of scans per spectrum.

3. Results and discussion

The fact, that the peak in $R(\omega, \varpi)$ is a sum of “matched” peaks from all spectra has important consequences for the sensitivity. As shown in Fig. 2, even if in a series of N spectra each one is too noisy for it to be possible to effectively pick some of the peaks (such as H^N resonances at 8–8.5 ppm), the RT, since it has $\sqrt{N} \times$ higher sensitivity is able to reveal all of them. This is particularly important in the case of unstable samples at low concentrations, where measurements have to be quick.

Fig. 2C shows the sensitivity on the example of Asn-5 resonance. Interestingly, the doublet is slightly worse resolved than in reference “perfect data” (red line). This can be explained by the fact, that ϖ grid does not contain the exact value of shift rate for Asn-5. Original paper on PROSPECT [6] suggested to use two additional processing techniques in RT spectra: sinebell multiplication and “shearing” yielding peaks of shape more similar to that known from multidimensional frequency-domain spectra. Although the modification can be useful in some cases, we did not find it appropriate in our study. Sinebell multiplication leads to obvious sensitivity loss, which is not desired, especially in the context of the current paper. Shearing provides RT spectra where peaks are centred at ω corresponding to the middle of temperature range, rather than the beginning. In our opinion, for practical reasons, it is better to have the initial spectrum as a reference. Anyway, shearing does not allow to extract any additional information from the spectra.

These benefits offered by RT are even more significant in serial 2D measurements, as multidimensional spectroscopy is naturally less sensitive. Moreover, as shown above, well resolved peaks in the frequency domain provide good resolution in the ϖ dimension.

Fig. 3 and a video in SI show the result of RT processing for a series of ^{15}N -HSQC of oxytocin. In this case, the shift is assumed only in ^1H dimension and thus the resulting spectrum is a three-dimensional object. The ϖ_0 coordinate of each peak can easily be found since it corresponds to a maximum intensity.

If the sensitivity is high enough, RT processing can provide the information normally provided by a series of 2D spectra in the time that a single 2D experiment would take. This is possible if the temperature (or any other factor causing the peak shift) is co-incremented with indirect time delays (see Fig. 4B).

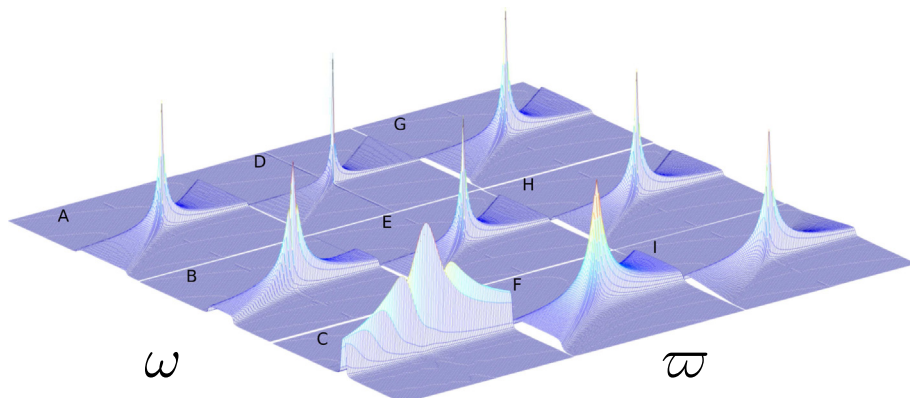


Fig. 1. Lineshape in the Radon transform of a series of M FID signals of amplitude A decaying exponentially in t at the rate $\Delta\varpi_{1/2}$. A,B,C – number of spectra influences linewidth in the ϖ dimension (A and $\Delta\varpi_{1/2}$ constant). A – $M = 100$; B – $M = 50$; C – $M = 10$; D,E,F – linewidth in ω influences the linewidth in ϖ dimension (A and M constant). D – $\Delta\varpi_{1/2} = 0.1$; E – $\Delta\varpi_{1/2} = 0.5$; F – $\Delta\varpi_{1/2} = 1.5$; G,H,I – effect of linear decrease of amplitude on the lineshape ($\Delta\varpi_{1/2}$ and M constant) G – $A = 1$; H – $A = 1 - 0.5 \cdot s$; I – $A = 1 - s$ ($s = 0, \dots, 1$).

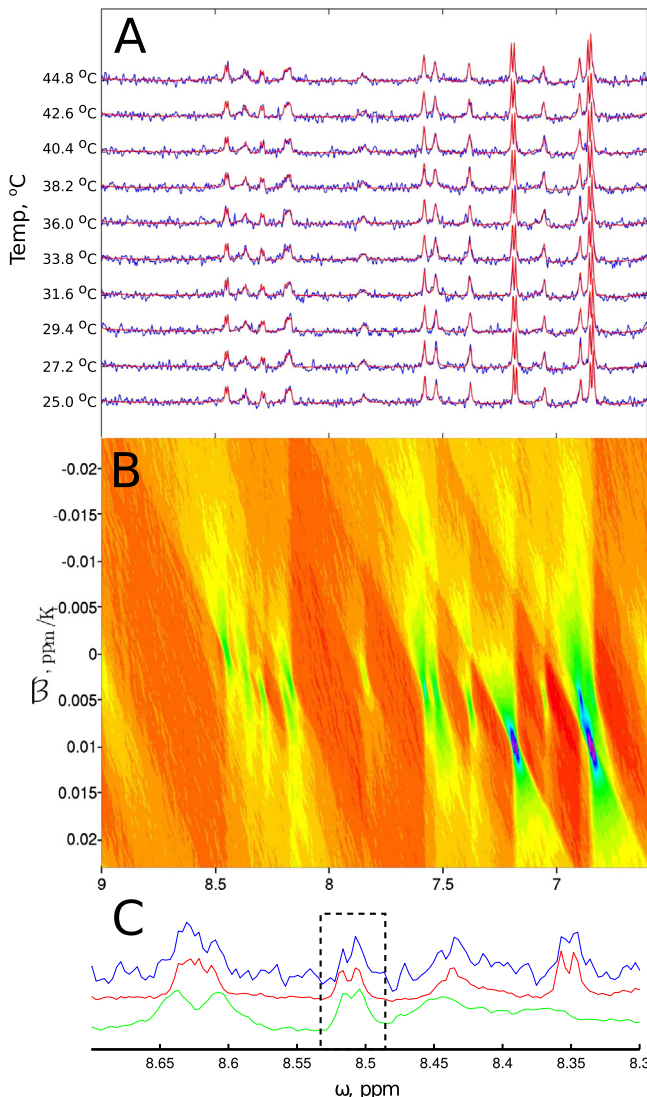


Fig. 2. Conventional series of 1D experiments vs. Radon transform experiment. Panel A: series of 1D spectra of oxytocin at temperatures from 25°C to 44.8°C (red – “perfect spectrum”, 256 scans; blue – with added noise). Panel B: spectrum obtained by Radon transform of a series of 200 1D spectra at temperatures from 25 °C to 45 °C with noise level $\sqrt{20} \times$ higher than in a “blue” series from panel A (and thus corresponding to equivalent experimental time). Panel C: The zoomed-in region from Panel A (spectra at 25 °C) with a 1D trace from Panel B at ϖ corresponding to the Asn-5 doublet (marked with the dashed line). Video showing all cross-sections is available in SI. (For interpretation of the references to colour in this figure legend, the reader is referred to the web version of this article.)

In fact, this corresponds to a radial sampling of the time-temperature space. Assuming that $\vec{t} = (t_1, t_2) \in \mathbb{R}^2$ and that with varying s the peaks move only along the direct spectral dimension, the signal becomes $g(t_1, t_2) = f(\alpha\varpi_1 t_1 + \omega_1) t_1 + (\alpha\varpi_2 t_1 + \omega_2) t_2)$. In this setting, the “semi-RT” can be defined as:

$$SR(\vec{\omega}, \vec{\varpi}) = \int g(\vec{t}) \exp(-2\pi i((\alpha\varpi_1 t_1 + \omega_1) t_1 + (\alpha\varpi_2 t_1 + \omega_2) t_2)) d^2 \vec{t}. \quad (6)$$

As seen in Fig. 5 the lineshapes outside the matching condition are different than those in the RT of the series of conventionally sampled 2D spectra in Fig. 3. In fact, their shape makes the manual location of maximum easier than in the conventional case. SI contains scripts generating lineshapes of “conventionally” and “radially” sampled RT spectra.

Extension of RT from 1D to higher dimensions deserves broader discussion. On the mathematical level, it boils down to the replacement of the scalar variable ϖ by a vector variable $\vec{\varpi}$. In the conventional sampling case (see Eq. (5)) the components of $\vec{\varpi}$ enter the formula in the symmetric way, whereas in the radial sampling the symmetry is broken (see Eq. (6)). Fig. 1 in SI shows the difference in lineshape in both ϖ dimensions of 4D ($\omega_1, \omega_2, \varpi_1, \varpi_2$) RT spectrum of radially sampled data. The peak’s shift in the co-incremented dimension causes lineshape effects similar to those observed in a Fourier analysis of signals with linearly varying frequency (linear chirps). Actually, such lineshapes have been long known in NMR, either caused by linearly varying B_0 field during acquisition of FID or the field-sweep in continuous-wave NMR (see e.g. [9]). Linearly varying frequency corresponds to $t_1^2 \varpi_1$ term in the exponent of Eq. (6) and it is known that in this case Fourier analysis should be replaced by the fractional Fourier analysis, that can provide absorptive lineshape for correct ω and ϖ , as defined in [10]. In fact, formula (6) resembles the fractional Fourier transform in t_1 . Remarkably, in both conventional and radial approach, when ϖ_1 and ϖ_2 match the actual shift rate of the peak, the 2D $\omega_1 - \omega_2$ cross-section of the 4D RT spectrum contains standard Lorentzian peak. Thus, both methods are applicable to study peak shifts in any of the spectral dimensions.

To verify the result of RT processing of “radially” sampled data we acquired a conventional set of 2D ^{15}N HSQC spectra at varying temperatures (25, 26, ..., 37 °C). Although the number of spectra is too small to provide good resolution in RT (as explained in Fig. 1A-C), it can be processed in a conventional way, i.e. positions of the peaks in each spectrum can be plotted against the temperature and ϖ can be found by a linear fit. The value of the directional coefficient of such fit for Ile-3 is 0.0104 ppm/K which matches quite well with the result obtained from “semi-RT”, i.e.

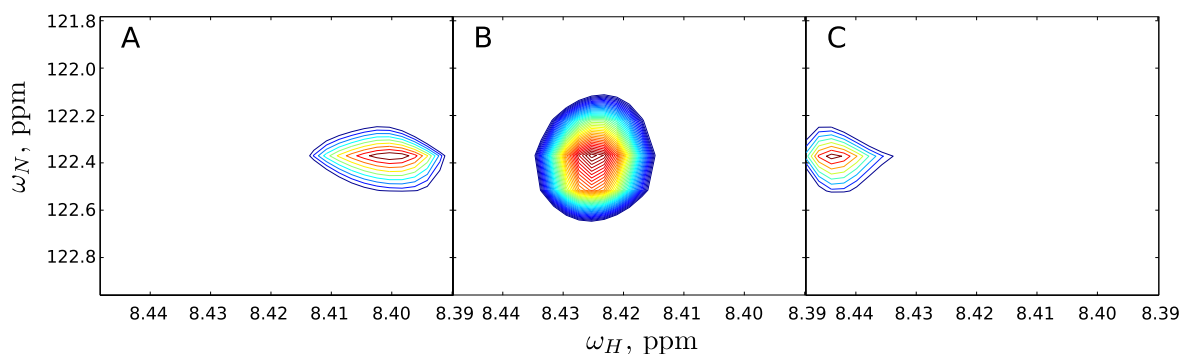


Fig. 3. Cross-sections showing Leu-8 resonance (shifts only in direct dimension) in the RT of “conventionally sampled” series of ^{15}N -HSQC of oxytocin A – outside the top of the RT peak in ω_H dimension, $\varpi_H = -0.0044$ ppm/K, B – on the top of the RT peak, $\varpi_H = 0.00059$ ppm/K, C – outside the top of the RT peak in ω_H dimension, $\varpi_H = 0.0066$ ppm/K. Video with all cross-sections and full spectrum available in SI.

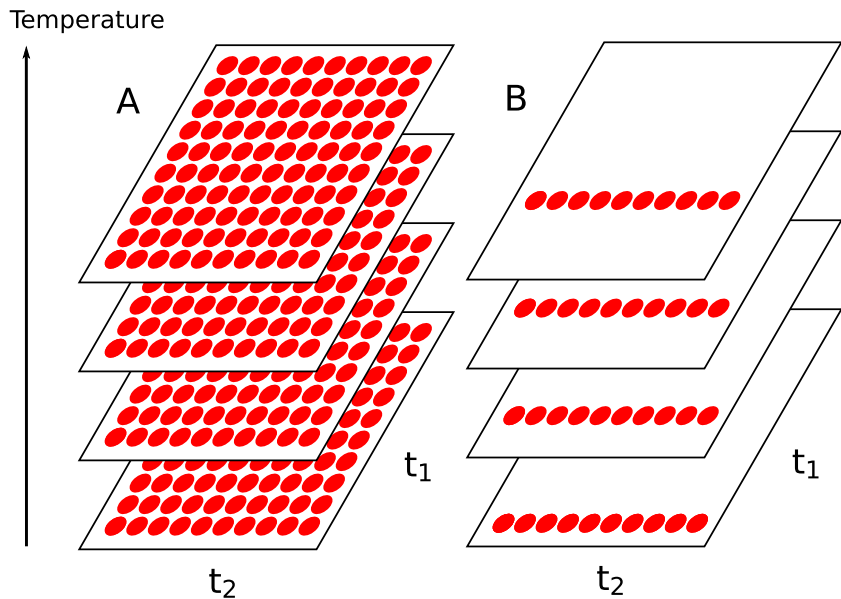


Fig. 4. Sampling in serial 2D experiments: A – conventionally sampled experiment repeated for every setting of temperature; B – “radial sampling” of the temperature-time domain. The temperature is co-incremented with indirect time t_1 .

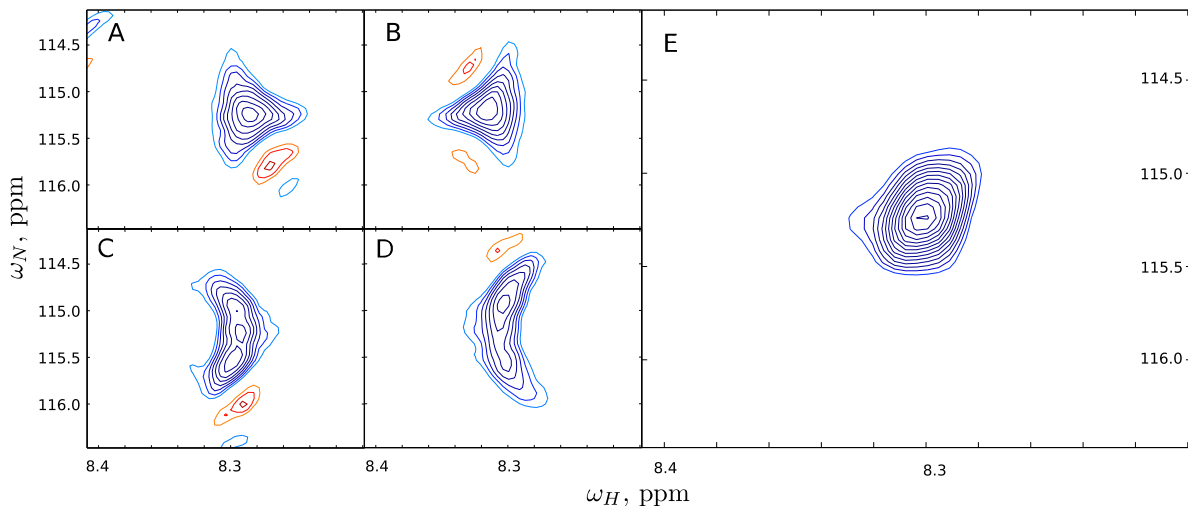


Fig. 5. 2D cross-sections showing Ile-3 resonance in RT of “radially sampled” series of ^{15}N -HSQC of ubiquitin. A,B,C,D – at various places outside the top of the RT peak: A – $\varpi_H = 0.0204 \text{ ppm/K}$, $\varpi_N = 0 \text{ ppm/K}$; B – $\varpi_H = 0.0 \text{ ppm/K}$, $\varpi_N = 0 \text{ ppm/K}$; C – $\varpi_H = 0.0103 \text{ ppm/K}$ (optimum), $\varpi_N = -0.0872 \text{ ppm/K}$; D – $\varpi_H = 0.0103 \text{ ppm/K}$ (optimum), $\varpi_N = 0.1390 \text{ ppm/K}$; E – Cross-section corresponding to the top of the peak in σ dimensions: $\varpi_H = 0.0103 \text{ ppm/K}$, $\varpi_N = 0.0259 \text{ ppm/K}$. Contour levels are the same for all panels. Video with all cross-sections of Ile-3 and larger fragment of a spectrum are available in SI.

$\varpi_H = 0.010299 \pm 0.0003 \text{ ppm/K}$ (the error is derived from the size of grid in ϖ_H dimension). Similarly good result (0.0277 ppm/K vs. $0.0259 \pm 0.0037 \text{ ppm/K}$) is obtained for ^{15}N dimension. The plots are shown in SI Fig. 2.

One may notice, that the “radial” sampling scheme resembles famous “accordion” experiment, where direct FT was applied to similar data and changes affecting peaks were deconvolved from their shapes [11]. Indeed, 2D cross-section from RT spectrum at ($\varpi_1 = 0, \varpi_2 = 0$) corresponds to 2D FT of the “accordion” data. Such processing provides peak-shapes like the one observed in Fig. 5B. Decoding the rate of peak shift by deconvolution is probably possible, but RT seems to be a far better approach. Firstly, it provides a sensitivity gain (compare peak heights in Fig. 5B and E). Secondly, it does not require a reference spectrum of a “static sample”, that is needed to separate other line-shape effects [12].

Importantly, both the “conventionally” sampled oxytocin experiment and the “radially” sampled ubiquitin experiment

provide significant time and sensitivity gains compared to the conventional approach, where the minimal dataset (assuming a linear change of peak coordinates) is two spectra acquired at the borders of the temperature range. Since each of them is processed separately, the signal-to-noise ratio is $\sqrt{2} \times$ lower. Also, with two spectra it is not possible detect any deviations from linearity or the critical (e.g., denaturation) temperature for the sample. Testing temperatures in small steps makes it possible to discover problems, and, if they arise, to process only a subset of data. In fact, even in the conventional approach (without RT), increasing the temperature in small steps is a common practice [13–15].

4. Experimental

Oxytocin (2 mg) was dissolved in 600 μl of 10:90 $\text{D}_2\text{O}/\text{H}_2\text{O}$ and transferred to 5 mm tube. ^1H NMR spectra were recorded with a

double pulse field gradient spin echo (dpgse) pulse sequence for water suppression (pulse sequence from Biopack, VnmrJ 4.2). 200 measurements were recorded at incremental temperatures from 25 °C to 45 °C. The experiments were carried out using an Agilent 700 MHz NMR spectrometer with an HCN room-temperature probe and DD2 console. 256 scans and 16,384 complex data points per FID were used, acquisition time of 0.24 s, pulse width 7.1 μs, spectral width 12,019 Hz and recycle delay of 1.5 s. The noise was added to the original spectrum to obtain datasets presented in Fig. 2.

A six times more concentrated oxytocin sample was used for a series of ¹⁵N-HSQC spectra (gNhsqc pulse sequence from Biopack, VnmrJ 4.2) with 100 *t*₁ increments and 8 scans per point. ¹⁵N pulse was 59 μs and the ¹⁵N spectral width was 4,257 Hz. Interscan delay was 1 s and the temperature sweep from 25° to 35 °C in steps of 0.1 °C.

2D measurements with co-incremented *t*₁ and temperature were carried out on a ¹⁵N-labelled ubiquitin sample (1 mM in 50 mM phosphate buffer, 10% D₂O, 0.02 % NaN₃, pH 7 obtained from Giotto Biotech). The experiment was performed with a gNhsqc pulse sequence with 256 *t*₁ increments. Each indirect sampling point was acquired with 4 scans and at an incremented temperature making the sweep from 25° to 37.8 °C. Spectral widths and pulse lengths were the same as in oxytocin experiment. A relaxation delay of 1 s was used. The temperature stabilization period of 15 s was used in all experiments.

In order to verify the result obtained from the RT on ubiquitin, the additional dataset has been acquired in conventional manner by measuring ¹⁵N HSQC spectra at temperatures 25, 26, ..., 37 °C.

The RT for all experiments assumed frequency shift in proton dimension only. The range of ϖ_H was as follows: for 1D oxytocin spectra [−0.022854, −0.022854] ppm/K (1592 grid points), for 2D oxytocin spectra [−0.013359, 0.013359] ppm/K (160 grid points), for 2D ubiquitin spectra [−0.033464, 0.033464] ppm/K (200 grid points).

All 2D spectra have been processed with 4× zero-filling in both dimensions for clear visualization. The FID was Fourier transformed in the direct dimension using nmrPipe [16], truncated to the amide region and inverse Fourier transformed back to the time domain. Such data was used as an input for the RT, which explains the peak folding effect on the borders of the RT spectrum in Fig. 2.

5. Conclusion

Using a Larmor frequency change model can help improve the sensitivity of serial NMR experiments. Radon transforms provide an opportunity for this improvement, treating a series of spectra with linearly moving peaks as a single object. A Radon transform decodes the rate of peak movement and provides spectral information with the same level of sensitivity as an experiment with constant peak positions run at the same time. Transforms revealing

changes other than linear are also possible, and will be studied in future research.

Acknowledgment

This work was supported by grants from National Science Centre of Poland: SONATA BIS (2012/07/E/ST4/01386) and OPUS (2015/17/B/ST4/04221).

Appendix A. Supplementary material

Supplementary data associated with this article can be found, in the online version, at <http://dx.doi.org/10.1016/j.jmr.2017.07.011>.

References

- [1] R.R. Ernst, W.A. Anderson, Application of Fourier transform spectroscopy to magnetic resonance, *Rev. Sci. Instrum.* 37 (1) (1966) 93–102.
- [2] J. Jeener, Ampere International Summer School, Basko Polje, Yugoslavia, 1971.
- [3] W.P. Aue, E. Bartholdi, R.R. Ernst, *Two-dimensional spectroscopy: application to nuclear magnetic resonance*, *J. Chem. Phys.* 64 (5) (1976) 2229–2246.
- [4] P.T. Callaghan, C.H. Arns, P. Galvosa, M.W. Hunter, Y. Qiao, K.E. Washburn, *Recent Fourier and Laplace Perspectives for Multidimensional NMR in Porous Media*, Oxford University Press, Cambridge, MA, 2011, <http://dx.doi.org/10.1016/j.mri.2007.01.114>.
- [5] P. Barone, A. Ramponi, G. Sebastiani, *On the numerical inversion of the Laplace transform for nuclear magnetic resonance relaxometry*, *Inverse Prob.* 17 (1) (2001) 77–94.
- [6] E. Kupče, R. Freeman, *Mapping molecular perturbations by a new form of two-dimensional spectroscopy*, *J. Am. Chem. Soc.* 135 (8) (2013) 2871–2874.
- [7] E. Kupče, R. Freeman, *The Radon transform: a new scheme for fast multidimensional NMR*, *Concepts Magn. Resonance Part A* 22A (1) (2004) 4–11.
- [8] S.R. Deans, *The Radon Transform and Some of its Applications*, Dover Publications, 2007.
- [9] B.A. Jacobsohn, R.K. Wangsness, *Shapes of nuclear induction signals*, *Phys. Rev.* 73 (1948) 942–946.
- [10] V. Namias, *The fractional order fourier transform and its application to quantum mechanics*, *IMA J. Appl. Math.* 25 (3) (1980) 241–265, <http://dx.doi.org/10.1093/imamat/25.3.241>.
- [11] G. Bodenhausen, R. Ernst, *The accordion experiment, a simple approach to three-dimensional spectroscopy*, *J. Magn. Reson.* 45 (1981) 367.
- [12] J. Balbach, V. Forge, W. Lau, N. van Nuland, K. Brew, C. Dobson, *Protein folding monitored at individual residues during a two-dimensional NMR experiment*, *Science* 274 (1996) 1161–1163.
- [13] R.E. Sallach, M. Wei, N. Biswas, V.P. Conticello, S. Lecommandoux, R.A. Dluhy, E. L. Chaikof, *Micelle density regulated by a reversible switch of protein secondary structure*, *J. Am. Chem. Soc.* 128 (36) (2006) 12014–12019.
- [14] A. Troganis, I.P. Gerothanassis, Z. Athanassiou, T. Mavromoustakos, G.E. Hawkes, C. Sakarellos, *Thermodynamic origin of cis/trans isomers of a proline-containing β-turn model dipeptide in aqueous solution: A combined variable temperature ¹H-NMR, two-dimensional ¹H,¹H gradient enhanced nuclear overhauser effect spectroscopy (NOESY), one-dimensional steady-state intermolecular ¹³C,¹H NOE*, *Biopolymers* 53 (1) (2000) 72–83.
- [15] L.R. Malins, J.N. DeGruyter, K.J. Robbins, P.M. Scola, M.D. Eastgate, M.R. Ghadiri, P.S. Baran, *Peptide macrocyclization inspired by non-ribosomal imine natural products*, *J. Am. Chem. Soc.* (2017) 5233–5241.
- [16] F. Delaglio, S. Grzesiek, G. Vuister, G. Zhu, J. Pfeifer, A. Bax, *NMRPipe: A multidimensional spectral processing system based on UNIX pipes*, *J. Biomol. NMR* 6 (3) (1995) 277–293.